Materials Chemistry and Physics

In-situ characterisation of the corrosion products formed on C-steel immersed in a soil-simulating solution

--Manuscript Draft--

Manuscript Number:	
Article Type:	Full Length Article
Keywords:	in-situ Raman spectroscopy; cathodic protection; corrosion in Soil; green rust
Corresponding Author:	Luca Casanova Milan, Italy ITALY
First Author:	Luca Casanova
Order of Authors:	Luca Casanova
	Marco Menegazzo
	Andrea Brenna
	MariaPia Pedeferri
	Lamberto Duò
	Marco Ormellese
	Gianlorenzo Bussetti
Abstract:	In this research C-steel corrosion products are allowed to form in a water-based solution containing 1000 ppm of SO42−, which simulates a highly corrosive soil. The electrode Fermi level was controlled with a three electrodes electrochemical set-up, scanning a potential window between the corrosion and the passivation regions. This, combined with in-situ Raman spectroscopy, allows to characterise the surface chemistry of the products formed according to the ongoing electrochemical reactions. When the potential is held in the stability region of the ionic species the surface state of the metal is characterised principally by the presence of lepidocrocite (γ-FeOOH) and green rust (GR-SO42−). The application of an anodic potential, simulating the effect of a DC anodic interference, combined with factors like moisture, presence of oxygen and sulphate ions contribute to develop a multicoloured (mix orange-like, yellow and green) mainly amorphous reaction product composed by a mix of iron oxide and oxi-hydroxide phases.
Suggested Reviewers:	Edoardo Proverbio eproverbio@unime.it
	Marina Cabrini marina.cabrini@unibg.it
	Sergio Lorenzi sergio.lorenzi@unibg.it
	Nick Birbilis nick.birbilis@anu.edu.au

In-situ characterisation of the corrosion products formed on C-steel immersed in a soil-simulating solution

L. Casanova[a]*, M. Menegazzo[b], A. Brenna[a], M. Pedeferri[a], L. Duò[b], M. Ormellese[a] and G. Bussetti[b]

[a]*Dept. of Chemistry, Materials and Chemical Engineering "G. Natta", Politecnico di Milano, Via Mancinelli 7, 20131 Milano, Italy*

[b]*Dept. of Physics, Politecnico di Milano, Piazza Leonardo Da Vinci, 20133 Milano, Italy*

**corresponding author: luca.casanova@polimi.it*

Abstract

In this research C-steel corrosion products are allowed to form in a water-based solution containing 1000 ppm of SO_4^{2-}, which simulates a highly corrosive soil. The electrode Fermi level was controlled with a three electrodes electrochemical set-up, scanning a potential window between the corrosion and the passivation regions. This, combined with in-situ Raman spectroscopy, allows to characterise the surface chemistry of the products formed according to the ongoing electrochemical reactions. When the potential is held in the stability region of the ionic species the surface state of the metal is characterised principally by the presence of lepidocrocite (γ-FeOOH) and green rust (GR-SO_4^{2-}). The application of an anodic potential, simulating the effect of a DC anodic interference, combined with factors like moisture, presence of oxygen and sulphate ions contribute to develop a multicoloured (mix orange-like, yellow and green) mainly amorphous reaction product composed by a mix of iron oxide and oxi-hydroxide phases.

Keywords: in-situ Raman spectroscopy; cathodic protection; corrosion in soil; green rust

Introduction

Buried carbon steel pipelines are extensively used infrastructures for the transport and distribution of hydrocarbons (as methane and oil) and water. As their corrosion generally implies high costs and dangerous inconvenience for the human health, a deep knowledge of the main forms of corrosion and how to mitigate them remains a subject of great importance. In order to preserve the structural integrity, one of the best choices is to combine a coating, composed by coal tar enamel or polymeric material, and a cathodic protection system (impressed current or sacrificial anodes). In absence of cathodic protection, corrosion may even occur in the form of a localised attack often leading to leakages[1]. Such local attacks may arise from cracks or inhomogeneities in

the iron oxide layer permitting an anode to form at the base of the discontinuity and a cathode to establish someway over the sample surface. Generally, the anodic and cathodic reactions of C-steel buried in an aerated neutral soil can be expressed by **Eq. 1** and **2**

$$2Fe \rightarrow 2Fe^{2+} + 4e^{-} \quad (1)$$

$$O_2 + 2H_2O + 4e^{-} \rightarrow 4OH^{-} \quad (2)$$

The driving force of the reaction causes iron cations migration away from the metal and accumulation of anions like Cl^- and OH^- until a cap of corrosion products, mainly composed of iron oxides, hydroxides or oxi-hydroxides, may form. Here the metal valence presents a mixed +2/+3 character (magnetite or green rust) or even +3 (hematite, lepidocrocite, goethite…) according to the oxidising environmental conditions. Among the most important factors affecting the aggressivity of the environment moisture, oxygen content, soil resistivity (dependent on dissolved salts), temperature, pH and eventual presence of bacteria rule the occurrence of the corrosion attack. However, even external factors such as stray currents, originating from AC or DC sources, may be relevant for the corrosion kinetics.

Electrochemical laboratory scale simulations, of the corrosion processes developing on the external pipe surfaces, may be afforded recreating the in-service conditions experienced by the materials using in-situ collected soil samples[2, 3] or simulating the soil composition according to properly designed liquid electrolytes. The latter, for sure, offer a simpler example of ease of implementation and availability. According to that Wu *et al.*[4] investigated the performance of Q235 steel in a solution containing NaCl, $CaCl_2$, Na_2SO_4, $MgSO_4$, $NaHCO_3$ and KNO_3 adjusting the pH between 3 and 7 with sulphuric acid in order to simulate acid deposits finding a corrosion reaction rate first order with the proton concentration. Liu *et al.*[5] prepared a 0.01 M NaCl based soil-simulating solution adding different salts. The author found that the addition of cations promoted higher corrosion rates following the order $K^+ > Mg^+ > Ca^{2+}$, while for the anions the following rule was validated $SO_4^{2-} > HCO_3^- > NO_3^-$. Also Benmoussa *et al.*[6] prepared a soil-simulating solution by adding the exact content of ions found in several samples of soil extracted in Algeria, finding the sulphate ion as the most concentrated specie. A similar approach was adopted by Belmokre *et al.*[7], using a criterion of soil aggressiveness based on the chloride and sulphate content, using higher concentrations for the latter anion. Sulphate salts are often present in ground water or feeding water of boilers[8] and are generally recognised to enhance the formation of pits over the steel surface, with pit density scaling with the sulphate concentration[9]. Based on those analysis and well established the participation of sulphates in the corrosion attack of C-steel, the

present study will be devoted to the in-situ characterisation of corrosion products formed on C-steel immersed in a soil-simulating solution, containing 1000 ppm of SO_4^{2-}, according to the use of Raman spectroscopy. This solution, provided the high humidity, the high sulphate content, the corrosion potential of C-steel and the low resistivity (8.285 Ω·m) should simulate a severe soil according to the "indices" model developed by Trabanelli[10] forecasting a corrosion rate >0.5 mm/year. The formation of surface films is investigated both at the corrosion potential (E_{corr}), and at a more positive value, i.e., +0.5 V/SHE (Standard hydrogen electrode), offering the opportunity of studying the surface state of anodic regions of buried structures subjected to stray currents originating from stationary or non-stationary sources[11–14]. These conditions may verify if the structure of interest interfere with the ground bed of a cathodic protection plant, or as a result of the dispersed current coming from a DC traction system.

Raman spectroscopy is a particularly useful surface technique for the in-situ characterisation of film produced according to electrochemical phenomena. Following a similar approach Odziemkowski *et al.*[15] characterised iron films produced in a carbonates based solution held at pH=9, finding magnetite (Fe_3O_4), with Raman signals at 546 and 665 cm^{-1}, and $Fe(OH)_2$ (545 and 3416 cm^{-1}) as the main species. However, other authors[16] expressed doubts about the consistency of the 546 cm^{-1} band of iron II hydroxide as the brucite like phase presents only lines at 260 and 407 cm^{-1}. This point of view is more likely as this phase possesses a low Raman scattering cross section and because of its intrinsic low thermodynamic stability, causing its conversion to magnetite according to the disproportionation reaction [15] in **Eq. 3**

$$3Fe(OH)_2 \rightarrow Fe_3O_{4\,(s)} + H_{2\,(g)} + H_2O_{(l)} \quad (3)$$

A relatively recent Raman characterisation of iron oxide and oxyhydroxides is reported by de Faria *et al.*[17] who investigated the effect of the artefacts induced by the laser power, finding a "safe" compromise using a red laser (633 nm) with an output power over the sample limited to 0.7 mW. Generally, few studies[18] are present in literature regarding the in-situ Raman characterisation of the surface state of iron when immersed in a solution containing sulphates, giving also no indication about the laser power delivered to the sample, creating doubts about possible interconversions among phases. The ex-situ analysis of corrosion products may preclude the opportunity to understand all the intermediate phases and reactions contributing to the formation of a final scale of rust. As a result, the present analysis has the aim of unifying the knowledge of the iron surface state when the metal is immersed in a soil simulating solution containing sulphates only. The goal is reached by performing in-situ Raman spectroscopy, in an electrochemical cell containing an aerated solution of 1000 ppm of SO_4^{2-}, using a 633 nm laser with a power delivered

to the sample of 0.7 mW. The potential is varied anodically between E_{corr} and +0.5 V/SHE in order to simulate an anodic interference condition.

Materials and methods

All the experiments are performed with circular (diameter 10 mm) C-steel samples with the chemical composition shown in **Tab. 1**.

Tab. 1 Elemental composition of the C-steel used in the present analysis (values are referred to wt.%).

C 156	Mn 403	Cr 267	Ni 225	Mo 386	Cu 327	Al 396	Fe
0.05	0.264	0.081	0.031	0.001	0.018	0.012	Balance

The microstructure of the metal, shown in **Fig. 1a**, is revealed almost fully ferritic using a Nital 5 solution (95 %v/v ethyl alcohol + 5 %v/v HNO_3).

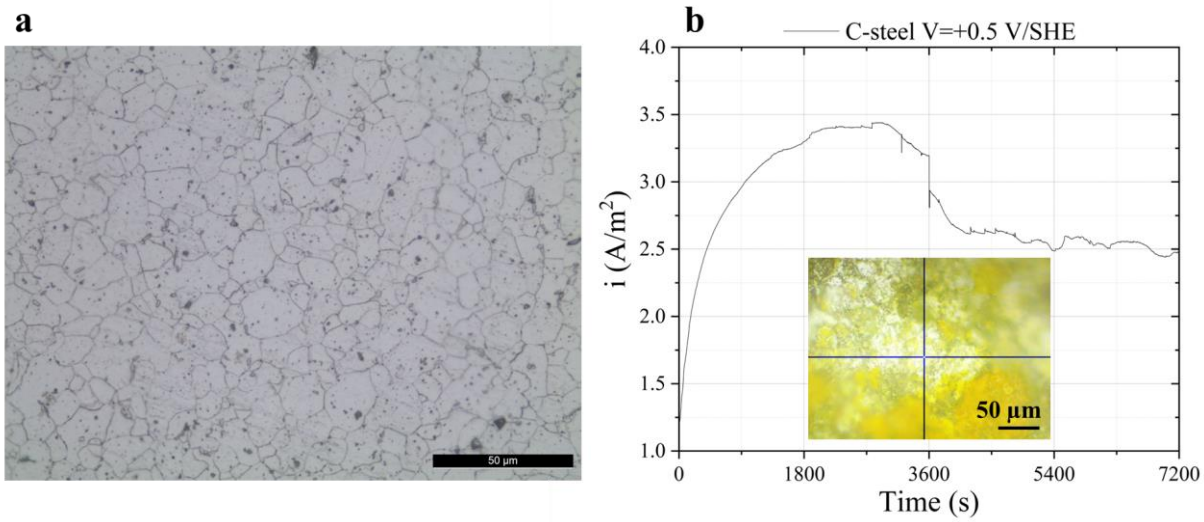

Fig. 1 a C-steel microstructure and **b** anodic current density of the steel undergoing DC interference at +0.5 V/SHE.

Samples are mechanically polished with silicon carbide papers and alumina particles to obtain a mirror like surface. Before the electrochemical experiments, samples are cleaned in ultrasound with acetone for 10 minutes and then washed in deionised water. After that, samples were immediately dried with nitrogen gas to preserve their surface state. All the electrochemical tests are performed using a Metrohm Autolab PGSTAT using a 4 ml PTFE 3 electrode cell (ASTM G5[19]) with a home-made KCl saturated silver-silver chloride reference electrode ($SSC_{sat.}$). All potential values are then converted with respect to a standard hydrogen electrode (SHE). The experiment is performed at a controlled temperature of 21 °C in an aerated solution of 1000 ppm of SO_4^{2-} using Na as the cation. The solution conductivity is 8.285 Ω·m with pH = 7. Potential is varied between E_{corr} (generally lying ~−0.45 V/SHE) and +0.50 V/SHE. In-situ Raman spectroscopy acquisitions are performed with a commercial NTEGRA Spectra set-up (NT-MDT), in correspondence of

previously mentioned potential values. Raman spectroscopy is performed by employing an excitation laser source at 532 nm, having a power of 5 mW. However, adjusting the ND filter at 1.4 allows the power delivered to the sample to be ~0.7 mW, low enough to avoid relevant phase transitions[17]. Crystal structure is characterized by x-ray diffraction using a Philips PW3020 goniometer with Cu $K_{\alpha 1}$ radiation (1.54058 Å) performed in Bragg-Brentano geometry. Corrosion products are investigated by means of scanning electron microscopy using a Carl Zeiss EVO 50VP SEM equipped with a Bruker x-ray spectrometer for chemical microanalysis (EDS).

Results and discussion

Immediately after immersion E_{corr} stabilises at about −0.45 V/SHE. After few hours the surface of the metal starts to cover with orange-like stains of corrosion products as demonstrated by the right image, present in **Fig. 2**, acquired by an optical microscope.

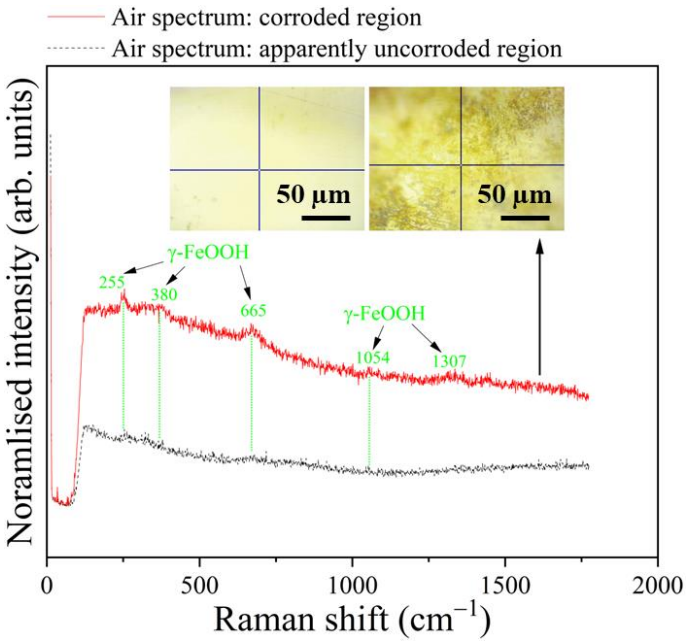

Fig. 2 Ex-situ Raman spectra of sample previously immersed in a 1000 ppm sulphate solution.

Removal of the sample from the testing solution and ex-situ Raman spectroscopy analysis reveals that in both apparently uncorroded and corroded regions, the main spectral features belong all to γ-FeOOH (lepidocrocite) with main peaks at 255, 380,1054 and 1307 cm^{-1}. Peak positions and relative intensities well agree with Raman spectrum present in several relevant studies[17, 20, 21]. The feature present at 665 cm^{-1} cannot be assessed rigorously as it can belong to lepidocrocite[20] - even if generally the peak is seen at 650 cm^{-1}- or can describe the more intense peak of magnetite (Fe_3O_4) as well. This is in agreement with the formation of corrosion products of iron in oxidising condition. From this preliminary analysis it appears that lepidocrocite is the main constituent forming after exposure, in free corrosion condition, to a solution containing sulphates.

After the C-steel permanence at E_{corr} for 2 h, the in-situ Raman spectra, shown in **Fig. 3**, present substantial differences with respect to previous data. In the low wavenumber region the plot is characterized by the overlapping of the peaks related to intermolecular translational vibrations of water[22, 23], whose modes are related to hydrogen bonding and additional effects pertaining to the surrounding environment[24].

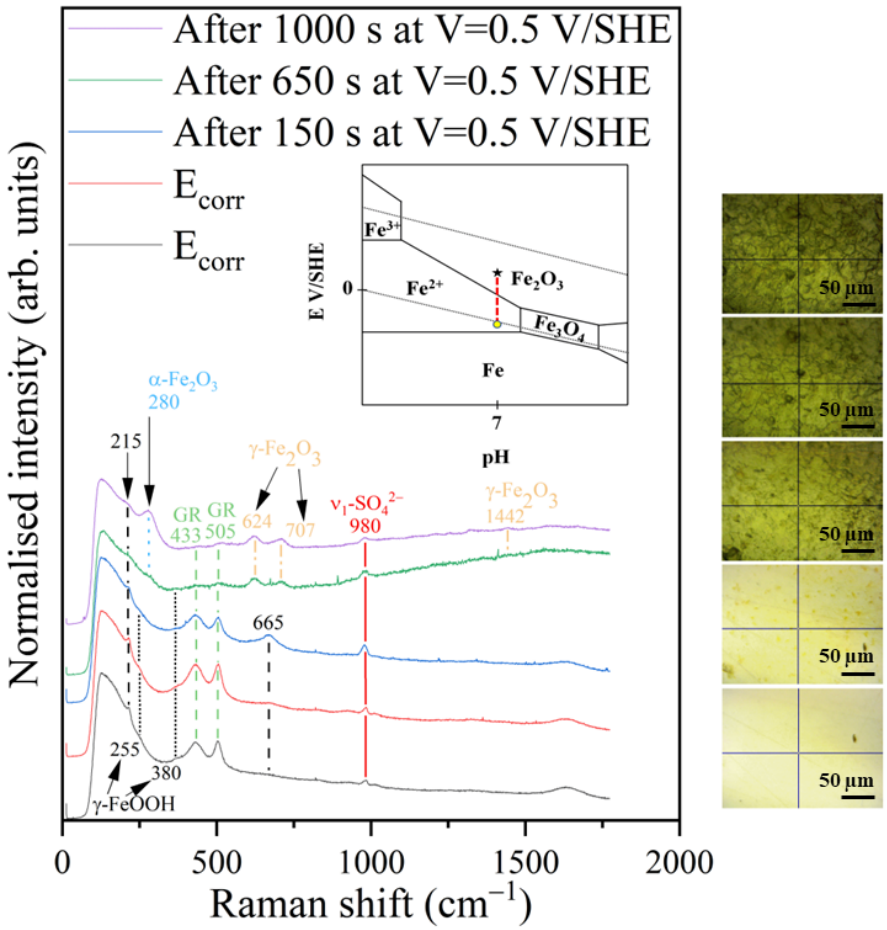

Fig. 3 Raman spectra characterising C-steel at E_{corr} and at an anodic potential of +0.5 V/SHE.

The last two liquid phase related Raman signals belong to the symmetric stretching of free sulphate ions (ν_1-SO_4^{2-} at ~980 cm^{-1}) and to the bending region of water (~1640 cm^{-1}).Apart from γ-FeOOH three features at 215, 433 and 505 cm^{-1} manifest. According to literature the last two lines should correspond to GR(SO_4^{2-}). The peaks at 433 and 505 cm^{-1} are assigned to the stretching of the Fe^{2+}-OH and Fe^{3+}-OH[25]. The ratio of the intensity is very close to unity, suggesting a similar amount of hydroxyl ions attached to Fe^{3+} and Fe^{2+}. On the other hand, difficulties arise from the assignment of the peak present at 215 cm^{-1}. According to Simard *et al.* [25] it should be related to the presence of Cl^- in GR an hypothesis automatically discarded due to the absence of the latter anion in the testing solution. Pineau *et al.* [26] obtained a GR(SO_4^{2-}) Raman spectrum much more similar to the one presented in this study even if the author did not justify the presence of the peak around 215 cm^{-1}. Another hypothesis is its relation to lepidocrocite, even if it is unexpectedly

higher than the major features present around 255 cm^{-1}. However, the disappearance of the peak at high anodic potential demonstrates that probably it describes an Fe^{2+}- related vibrational mode. This phase is generally observed in steel structures exposed to seawater or as the corrosion product of C-steel pipes devoted to water transport. Moreover it is generally recognised to be a source of sulphates for sulphates reducing bacteria (SRB)[26]. It is composed by layers of Fe^{2+}/Fe^{3+} oxyhydroxide, retaining an excess of positive charge, alternated by water molecules and SO_4^{2-} ions used to restore charge neutrality[26]. Even in seawater where the Cl^- to SO_4^{2-} concentration ratio is ~19, GR(SO_4^{2-}) is more abundant as the structure is more likely to form in presence of divalent anions. The absence of GR(SO_4^{2-}) in the ex-situ Raman spectrum, which was subjected to a similar immersion history, can be explained by the natural tendency seen for green rust to oxidise in favour of lepidocrocite in seawater[25–27]. This study demonstrates that the same effect can spontaneously occur in a soil-simulating environment. Moreover, the possibility of performing in-situ measurements permits to resolve structures sensible to atmospheric conditions like green rust. After 150 s of the application of an anodic potential (+0.5 V/SHE) the surface chemistry is practically unchanged, apart from few slight modifications, sign that the imposed oxidative conditions require some time to modify the electrode composition. Noteworthy is the noticeable increase of the normalised intensity of the stretching mode of sulphates correlating with the broadening observed at the GR(SO_4^{2-}) peaks at 433 and 505 cm^{-1}. The reasons behind this observation can be twice and possibly related to *1)* the release of sulphate ions accumulated in between the brucite-like layers of GR(SO_4^{2-})[26] and *2)* the accumulation of sulphates according to the anodic electrification of the electrode. At this point, also the peak at 665 cm^{-1} grows in intensity. As this features was previously observed in the air exposed sample its presence should not be strictly related to the application of the anodic potential but rather to the permanence in the testing solution. Moreover, the fact that it grows in intensity irrespectively of the other lepidocrocite peaks should be an indication that this feature is describing a vibrational mode related to another phase. Focusing on the anodic current density, seen in **Fig. 1b**, the causes related to its progressively increasing trend may be twice and *1)* dependent on the increase of surface concentration of sulphates, as demonstrated by Raman and in agreement with accepted models[28] indicating a soil aggressiveness proportional to the sulphates content, but also *2)* as the result of the hydrolysis of the Fe^{2+} cations, produced by the anodic reaction, determining a modification of the surface pH towards lower values.

Substantial changes start after 650 s of polarisation. In particular, the previously observed peaks belonging to GR(SO_4^{2-}) are progressively suppressed in favour of the formation of features related to Fe^{3+} bearing passivation products perfectly in agreement with the Pourbaix diagram shown in the insert of **Fig. 3**. However, given the high spatial inhomogeneity of the corrosion product, the anodic

current density still continues to increase in time, as shown in **Fig. 1b**. Accordingly, hematite, the most stable iron ore, and maghemite dominate the Raman spectra[17, 18, 29, 30]. At this point the anodic current density starts to decrease only when the surface coverage of stable Fe^{3+} phases, γ-FeOOH and δ-FeOOH, reaches high values. A possible observation that should favour the assignment of the 665 cm^{-1} feature to magnetite resides in its fading tendency in relation to the external applied potential. In fact, the oxidative condition, imposed by the anodic potential, guarantees the conversion of almost all the Fe^{2+} cations present in magnetite into Fe^{3+} ions, inducing the complete conversion of the spinel structure into γ-Fe_2O_3. This is plausible as the present applied potential is verified to be sufficient for the complete oxidation of Fe^{2+} cations contained in magnetite, presenting a redox potential dependent on the Fe^{2+}/Fe^{3+} stoichiometric ratio[27]. After the permanence in the electrochemical cell at +0.5 V/SHE for 2 h a voluminous orange-like scale of corrosion products, formed after 1 h of anodic polarisation and responsible for the decrease observed in the anodic current density (**Fig. 1b**), develops over the metallic material. In-situ Raman analysis are presented in **Fig. 4**, allowing to assess the various layers composing the corrosion product. Raman spectrum collected in correspondence of the darker regions shown in the insert 1 of **Fig. 4** perfectly agree with the spectrum of δ-FeOOH acquired by De Faria *et al.* [17] even if few features belonging to lepidocrocite can still be detected. On the other hand, brighter regions of the electrode surface, as in the insert 2 of **Fig. 4**, present all the previous specroscopic features observed for lepidocrocite. To confirm the structural constituents composing the reaction products, Raman spectrum 3 is acquired in the insert 3 of **Fig. 3** where an evident orange layer of lepidocrocite covers the darker layer previously verified to be constituted of δ-FeOOH.

The simulataneous presence of Fe_3O_4, γ-FeOOH and GR(SO_4^{2-}) is not new as McGill *et al.* [31] observed their formation upon corrosion of cast iron in water, while Boucherit *et al.* [32] found GR formation in correspondence of pitted regions.

Consequently the resulting spectrum (3) presents features belonging to both phases, allowing to say that the complex rust layer formed according to the present experimental procedure may be constitued by a first layer of lepidocrocite in contact with iron, a second layer of darker δ-FeOOH surmounted by a valuminous orange-like layer of lepidocrocite. Those phases may be the result of hydration of previously detected Fe^{3+} oxides[33]. Ex-situ analysis are carried out to confirm previous Raman observations collected in **Fig. 4**. SEM micrographs, in **Fig.s 5a** and **5b**, highlight several spherically-shaped structures which according to literature[34] should correspond to γ-FeOOH. Apart from Fe and O elements, which characterise the surface of the sample, no S detection results from EDS analysis. This is not strange as also Pineau *et al.* [26] observed that S

tends to accumulate in the intermediate region of the rust layer where the EDS probe can not be particularly sensitive. According to SEM micrograph no indication of GR is observed as the latter phase generally presents an esagonal platelet like shape[34]. X-ray diffraction analysis confirms the presence of lepidocrocite as the main phase covering the electrode surface. No δ-FeOOH can be distinguished probably because of amorphicity and overall lower content with respect to lepidocrocite. Peaks are very broad and considerably less intense than the one belonging to the substrate, sign that the iron oxi-hydroxides have a low degree of crystallinity, compatible with observation of others[34].

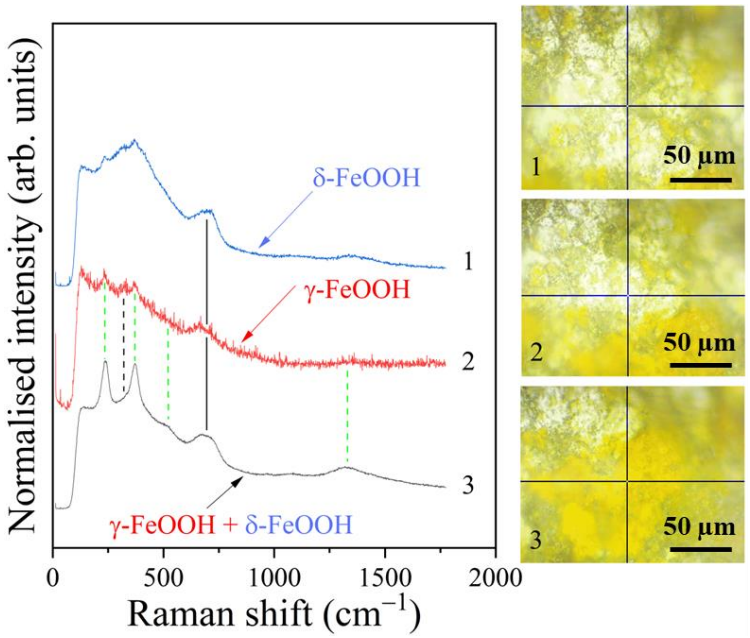

Fig. 4 Raman spectra acquired on C-steel after 2 h of polarisation at +0.5 V/SHE in different regions.

The absence of green rust related peak is justified by the great tendency of this phase to undergo fast oxidation leading to the formation of lepidocrocite, magnetite and goethite[26].

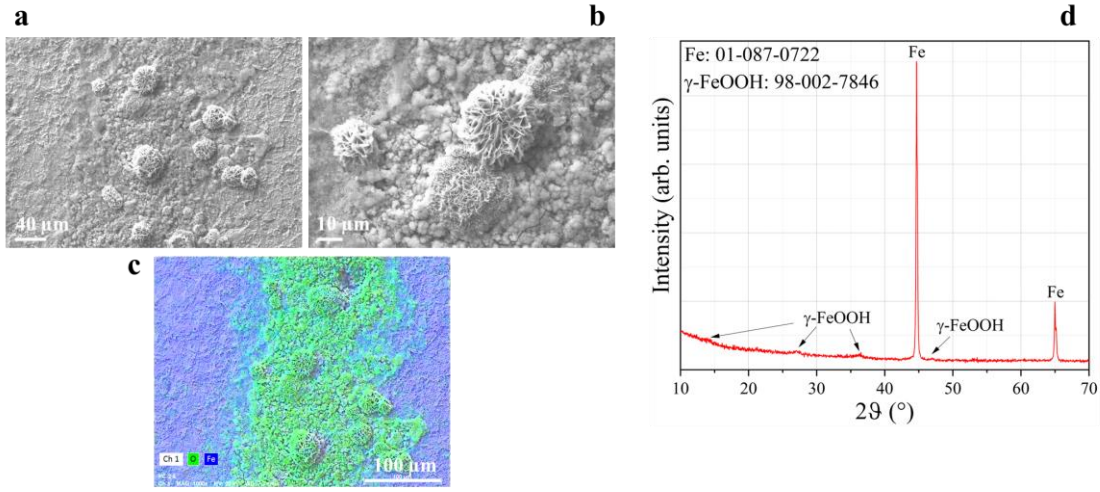

Fig. 5 SEM micrographs **a** and **b** of C-steel highlighting the corrosion product; **c** EDS map of Fe (blue) and oxygen (green) and **d** diffractogram of the corrosion products.

This demonstrates the great advantage of performing in-situ analysis permitting to detect GR in the first instant of its formation. This evidence is also supported by the study of other authors[35] observing the formation of GR according to the Fe corrosion in soil presenting O-deficient conditions.

Conclusions

Sulphate ions are a very common source of iron corrosion when the metal is employed in buried applications. Knowing the precise nature of the corrosion products, present over the metal surface, and their protectiveness may be of interest for techniques applied to preserve metallic structures like cathodic protection. For this aim, in-situ Raman spectroscopy demonstrates to be a useful technique for investigating the formation of local surface corrosion products which can be spatially resolved according to the use of an optical microscope immersed in the testing solution. According to the present experimental procedure the following conclusions can be drawn:

1. *Ex-situ analysis* of the corrosion product formed over C-steel immersed in a neutral solution containing sulphates allows to distinguish lepidocrocite (γ-FeOOH) as the main phase;
2. *In-situ Raman analysis* permits to detect the formation of reactive intermediate products, as green rust containing intercalated sulphate anions;
3. *Application of an anodic potential*, capable of simulating a condition of anodic DC interference, permits to study the time dependent evolution of the surface state of the electrode. As a result of the imposed oxidative condition, green rust, magnetite and lepidocrocite are initially converted to Fe^{3+} oxides like hematite (α-Fe_2O_3) and maghemite (γ-Fe_2O_3). For the first hour of polarisation the anodic current denotes a progressively increasing trend found to be related to an increasing surface concentration of sulphate, as demonstrated by Raman spectroscopy, and to a lower pH expected by the hydrolysis of the iron cation present in solution;
4. *After 2 h of permanence of the sample at +0.5 V/SHE* in aqueous solution a complex rust layer composed by a first layer of lepidocrocite in contact with the metal, a second darker layer of δ-FeOOH and a final voluminous orange-like reaction products of lepidocrocite form. This product, responsible to partially decrease the anodic current, is characterized to be mainly amorphous, presenting spherically-shaped structures typical of lepidocrocite.

Acknowledgements:
This work was carried out at the Solinano-∑ laboratory, a facility located at the Department of Physics of Politecnico di Milano.

Author contributions:
L. Casanova. Conceptualization, experimental design, data collection, editing, writing. **M. Menegazzo.** Experimental design, data collection, experimental design. **A. Brenna.** Editing, writing, experimental design. **M. Pedeferri.** Editing, writing. **L. Duò.** Editing, writing. **M. Ormellese.** Editing, writing, experimental design. **G. Bussetti.** Editing, writing, conceptualization, experimental design, data collection.

Conflicts of interest or competing interests:
The authors declare that they have no known competing financial interests or personal relationships that could have appeared to influence the work reported in this paper.

Data and code availability:
The data presented in this study are available on request from the corresponding author.

Supplementary information:
Not Applicable.

Ethical approval:
Not Applicable.

Bibliography
[1] Cole IS, Marney D, (2012) The science of pipe corrosion: A review of the literature on the corrosion of ferrous metals in soils. Corros Sci 56: 5–16

[2] Kasahara K, Kajiyama F, (1983) Determination of Underground Corrosion Rates From Polarization Resistance Measurements. Corrosion 39: 475–480

[3] Nie XH, Li XG, Du CW, Cheng YF, (2009) Temperature dependence of the electrochemical corrosion characteristics of carbon steel in a salty soil. J Appl Electrochem 39: 277–282

[4] Wu YH, Liu TM, Luo SX, Sun C, (2010) Corrosion characteristics of Q235 steel in simulated Yingtan soil solutions. Materwiss Werksttech 41: 142–146

[5] Liu TM, Wu YH, Luo SX, Sun C, (2010) Effect of soil compositions on the electrochemical corrosion behavior of carbon steel in simulated soil solution. Materwiss Werksttech 41: 228–233

[6] Benmoussa A, Hadjel M, Traisnel M, (2006) Corrosion behavior of API 5L X-60 pipeline steel exposed to near-neutral pH soil simulating solution. Mater Corros 57: 771–777

[7] Belmokre K, Azzouz N, Kermiche F, Wery M, Pagetti J, (1998) Corrosion study of carbon steel protected by a primer, by electrochemical impedance spectroscopy (EIS) in 3 % NaCI medium and in a soil simulating solution. Mater Corros - Werkstoffe und Korrosion 49: 108–113

[8] Bai B, Xiao G, Deng L, Zhang N, Chen C, Bu Y, Che D, (2021) A study on corrosion behavior of 15CrMo in saturated saline steam with sodium sulfate. Corros Sci 181: 109240

[9] Cavalcanti E, Wanderley VG, Miranda TR V., Uller L, (1987) The effect of water, sulphate and pH on the corrosion behaviour of carbon steel in ethanolic solutions. 32: 935–937

[10] Lazzari L, Pedeferri P, Ormellese M, (2006) Cathodic protection. First edit. Milan, 392 p

[11] Ormellese M, Brenna A, Lazzari L, Brugnetti F, (2014) Effects of anodic interference on carbon steel

under cathodic protection condition Experimental. In: Proc. Int. Conf. Eurocorr14, Eur. Fed. Corros. Event No. 364. Pisa, p 8

[12] Attarchi M, Brenna A, Ormellese M, (2020) Cathodic protection and DC non-stationary anodic interference. J Nat Gas Sci Eng 82: 103497

[13] Messinese E, Casanova L, Paterlini L, Capelli F, Bolzoni F, Ormellese M, Brenna A, (2022) A Comprehensive Investigation on the Effects of Surface Finishing on the Resistance of Stainless Steel to Localized Corrosion. Metals (Basel) 12: 1751

[14] Casanova L, Belotti N, Pedeferri M, Ormellese M, (2021) Sealing of porous titanium oxides produced by plasma electrolytic oxidation. Mater Corros 72: 1894–1898

[15] Odziemkowski MS, Schuhmacher TT, Gillham RW, Reardon EJ, (1998) Mechanism of oxide film formation on iron in simulating groundwater solutions: Raman spectroscopic studies. Corros Sci 40: 371–389

[16] Lutz HD, Möller H, Schmidt M, (1994) Lattice vibration spectra. Part LXXXII. Brucite-type hydroxides M(OH)2 (M = Ca, Mn, Co, Fe, Cd) - IR and Raman spectra, neutron diffraction of Fe(OH)2. J Mol Struct 328: 121–132

[17] De Faria DLA, Venâncio Silva S, De Oliveira MT, (1997) Raman microspectroscopy of some iron oxides and oxyhydroxides. J Raman Spectrosc 28: 873–878

[18] Gui J, Devine TM, (1994) The influence of sulfate ions on the surface enhanced raman spectra of passive films formed on iron. Corros Sci 36: 441–462

[19] (2014) ASTM G5 Standard Reference Test Method for Making Potentiodynamic Anodic Polarization Measurements. Annu B ASTM Stand. doi: 10.1520/G0005-13E02.2

[20] Hanesch M, (2009) Raman spectroscopy of iron oxides and (oxy)hydroxides at low laser power and possible applications in environmental magnetic studies. Geophys J Int 177: 941–948

[21] Hedenstedt K, Bäckström J, Ahlberg E, (2017) In-Situ Raman Spectroscopy of α- and γ-FeOOH during Cathodic Load. J Electrochem Soc 164: H621–H627

[22] Walrafen GE, Chu YC, Piermarini GJ, (1996) Low-frequency Raman scattering from water at high pressures and high temperatures. J Phys Chem 100: 10363–10372

[23] Abe K, Shigenari T, (2011) Raman spectra of proton ordered phase XI of ICE I. Translational vibrations below 350 cm-1. J Chem Phys. doi: 10.1063/1.3551620

[24] Tsai KH, Wu TM, (2006) Local structural effects on low-frequency vibrational spectrum of liquid water: The instantaneous-normal-mode analysis. Chem Phys Lett 417: 389–394

[25] Simard S, Odziemkowski M, Irish DE, Brossard L, Ménard H, (2001) In situ micro-Raman spectroscopy to investigate pitting corrosion product of 1024 mild steel in phosphate and bicarbonate solutions containing chloride and sulfate ions. J Appl Electrochem 31: 913–920

[26] Pineau S, Sabot R, Quillet L, Jeannin M, Caplat C, Dupont-Morral I, Refait P, (2008) Formation of the Fe(II-III) hydroxysulphate green rust during marine corrosion of steel associated to molecular detection of dissimilatory sulphite-reductase. Corros Sci 50: 1099–1111

[27] Usman M, Byrne JM, Chaudhary A, Orsetti S, Hanna K, Ruby C, Kappler A, Haderlein SB, (2018) Magnetite and Green Rust: Synthesis, Properties, and Environmental Applications of Mixed-Valent Iron Minerals. Chem Rev 118: 3251–3304

[28] Duranti F, Lazzari L, Marelli F, Tani S, (2010) Valutazione dello stato di corrosione di tubazioni interrate in acciaio in presenza di correnti vaganti. Metall Ital 102: 41–45

[29] Vind J, Malfliet A, Bonomi C, Paiste P, Sajó IE, Blanpain B, Tkaczyk AH, Vassiliadou V, Panias D, (2018) Modes of occurrences of scandium in Greek bauxite and bauxite residue. Miner Eng 123: 35–

[30] Chourpa I, Douziech-Eyrolles L, Ngaboni-Okassa L, Fouquenet JF, Cohen-Jonathan S, Soucé M, Marchais H, Dubois P, (2005) Molecular composition of iron oxide nanoparticles, precursors for magnetic drug targeting, as characterized by confocal Raman microspectroscopy. Analyst 130: 1395–1403

[31] McGill IR, McEnaney B, Smith DC, (1976) Crystal structure of green rust formed by corrosion of cast iron. Nature. doi: 10.1038/259200a0

[32] Boucherit N, Hugot-Le Goff A, Joiret S, (1991) Raman studies of corrosion films grown on Fe and Fe-6Mo in pitting conditions. Corros Sci 32: 497–507

[33] Cudennec Y, Lecerf A, Cudennec Y, Lecerf A, (2020) Topotactic transformations of goethite and lepidocrocite into hematite and maghemite To cite this version : HAL Id : hal-02537313 Solid State Sciences Volume 7 Issue Yannick Cudennec *, André Lecerf.

[34] Roh Y, Elless MP, (2018) Characterization of corrosion products in the permeable reactive. Environ Earth Sci 40: 184–194

[35] Halevy I, Alesker M, Schuster EM, Popovitz-Biro R, Feldman Y, (2017) A key role for green rust in the Precambrian oceans and the genesis of iron formations. Nat Geosci 10: 135–139

Declaration of interests

☑ The authors declare that they have no known competing financial interests or personal relationships that could have appeared to influence the work reported in this paper.

☐The authors declare the following financial interests/personal relationships which may be considered as potential competing interests:

Luca casanova
Marco Menegazzo
Andrea Brenna
MariaPia Pedeferri
Marco Ormellese
Lamberto Duò
Gianlorenzo Bussetti

In-situ characterisation of the corrosion products formed on C-steel immersed in a soil-simulating solution

L. Casanova[a]*, M. Menegazzo[b], A. Brenna[a], M. Pedeferri[a], L. Duò[b], M. Ormellese[a] and G. Bussetti[b]

[a]*Dept. of Chemistry, Materials and Chemical Engineering "G. Natta", Politecnico di Milano, Via Mancinelli 7, 20131 Milano, Italy*

[b]*Dept. of Physics, Politecnico di Milano, Piazza Leonardo Da Vinci, 20133 Milano, Italy*

**corresponding author: luca.casanova@polimi.it*

Cover Letter

Dear Editor of the journal *Materials Chemistry and Physics*,

we submit the manuscript entitled "*In-situ characterisation of the corrosion products formed on C-steel immersed in a soil-simulating solution*" to be considered for publication in your journal. The research is original, it was not previously published in other journals and data have not been presented in conferences or are under considered to other publications. The article has been written by the stated authors who are ALL aware of its content and approve its submission. No conflict of interest exists. If accepted, the article will not be published elsewhere in the same form, in any language, without the written consent of the publisher.

In the manuscript, we focus the investigation on the iron surface evolution during permanence in a soil-simulating solution. Despite being widely investigated, there is still not a general consensus about the precise nature of the corrosion products formed over the electrode when immersed in solution in free corrosion or when the metal is anodically polarised to simulate a direct current interference condition, often verified in practical applications. Using in-situ Raman spectroscopy we definitely prove that in free corrosion, the metal covers by a layer of green rust containing intercalated sulphate ions while in presence of anodic polarisation previous products are initially converted to hematite, maghemite and lepidocrocite.

We believe that this research can give a tangible contribution to both the scientific and the industrial sector, particularly if we consider those involved in corrosion mitigation techniques like cathodic protection, a technique widely applied and mandatory in case of pipelines used for the transport of natural gas and gaseous hydrogen. Last but not least, the research topic discussed in the manuscript can join the interest of the wide readers community of your journal.

Best regards,

Luca Casanova on the behalf of the co-authors